Received: 29 April 2022 | Revised: 4 July 2022 | Accepted: 14 July 2022

DOI: 10.1111/omi.12382

ORIGINAL ARTICLE

WILEY

A reappraisal of microbiome dysbiosis during experimental periodontitis

Marion Arce[1,2,3] | Natalia Endo[1,2] | Nicolas Dutzan[1,2,3] | Loreto Abusleme[1,2,4]

[1]Laboratory of Oral Microbiology, Faculty of Dentistry, University of Chile, Santiago, Chile

[2]Laboratory for Craniofacial Translational Research, Faculty of Dentistry, University of Chile, Santiago, Chile

[3]Department of Conservative Dentistry, Faculty of Dentistry, University of Chile, Santiago, Chile

[4]Department of Pathology and Oral Medicine, Faculty of Dentistry, University of Chile, Santiago, Chile

Correspondence
Loreto Abusleme Ramos, Department of Pathology and Oral Medicine, Faculty of Dentistry, University of Chile, Olivos 943, Independencia, Santiago, Chile.
Email: loreto.abusleme@odontologia.uchile.cl

Funding information
ANID, FONDECYT, Grant/Award Numbers: 11180505, 11180389; Scholarship, Grant/Award Number: 21221003

Periodontitis is a chronic inflammatory disease associated with the presence of dysbiotic microbial communities. Several studies interrogating periodontitis pathogenesis have utilized the murine ligature-induced periodontitis (LIP) model and have further examined the ligature-associated microbiome relying on 16S rRNA-based sequencing techniques. However, it is often very challenging to compare microbial profiles across studies due to important differences in bioinformatic processing and databases used for taxonomic assignment. Thus, our study aim was to reanalyze microbiome sequencing datasets from studies utilizing the LIP model through a standardized bioinformatic analysis pipeline, generating a comprehensive overview of microbial dysbiosis during experimental periodontitis.We conducted a reanalysis of 16S rDNA gene sequencing datasets from nine published studies utilizing the LIP model. Reads were grouped according to the hypervariable region of the 16S rDNA gene amplified (V1-V3 and V4), preprocessed, binned into operational taxonomic units and classified utilizing relevant databases. Alpha- and beta-diversity analyses were conducted, along with relative abundance profiling of microbial communities.

Our findings revealed similar microbial richness and diversity across studies and determined shifts in microbial community structure determined by periodontitis induction and study of origin. Clear variations in the relative abundance of bacterial taxa were observed starting on day 5 after ligation and onward, consistent with a distinct microbial composition during health and experimental periodontitis. We also uncovered differentially represented bacterial taxa across studies, dominating periodontal health and LIP-associated communities.

Collectively, this reanalysis provides a unified overview of microbial dysbiosis during the LIP model, providing new insights that aim to inform further studies dedicated to unraveling oral host–microbial interactions.

KEYWORDS
16S rRNA, 16S rDNA, dysbiosis, experimental periodontitis, ligature-induced periodontitis, microbiome

Abbreviations: LIP, Ligature-Induced periodontitis; 16S rRNA, 16S ribosomal RNA; 16S rDNA, 16S ribosomal RNA gene; NCBI, National Center For Biotechnology Information; RDP, Ribosomal Database Project; OTU, Operational Taxonomic Unit; MOMD, Mouse Oral Microbiome Database; PCoA, Principal Coordinates Analysis.

Marion Arce and Natalia Endo contributed equally to this study.

1 | INTRODUCTION

Periodontitis is a chronic inflammatory disease associated with the presence of dysbiotic microbial communities, and it is characterized by the destruction of tooth-supporting structures, which may lead to tooth loss (Papapanou et al., 2018). The polymicrobial nature of the microbiome instigating periodontitis is now widely accepted, contributing to the paradigm shift proposed for periodontitis etiology, currently understood as a dysbiotic condition rather than a classical infection (Curtis et al., 2020). The concept of dysbiosis refers to an altered state of the microbial community in terms of compositional and functional changes triggered by host-related and environmental factors that surpass the capacity of these communities to adapt, leading to an established microbial shift (Levy et al., 2017; Tiffany & Baumler, 2019). A series of clinical studies have revealed the profound microbiome alterations that underlie human periodontitis, including distinct shifts in microbial composition and structure, gene expression, metabolic and proteomic features, which have been analyzed in detail through the lens of next-generation sequencing approaches (Abusleme et al., 2013; Bao et al., 2020; Duran-Pinedo et al., 2014; Griffen et al., 2012). To provide more mechanistic insights into the role of these dysbiotic microbial communities during periodontitis, animal models, especially the mouse as a model organism, have made a critical contribution (Hajishengallis et al., 2015). In particular, the murine ligature-induced periodontitis (LIP) model has been widely utilized, and it consists of the placement of a silk ligature around the second maxillary molar, allowing the accumulation of native oral communities to occur on the ligature, which then triggers inflammatory alveolar bone loss within days (Abe & Hajishengallis, 2013). One of the most important features of this model is the opportunity to examine dysbiosis of an indigenous oral microbiome that has coevolved with the murine host without any manipulation other than placing the ligature. The recognition of the importance of these microbiome shifts in the context of various research questions that utilize the LIP model has prompted several studies to analyze in detail these microbial communities, relying mostly on 16S rRNA-based sequencing techniques (Dutzan et al., 2018; Hoare et al., 2021; Johnstone et al., 2021; Kitamoto et al., 2020; Kittaka et al., 2020, 2019; Tsukasaki et al., 2018; Williams et al., 2020; Zheng et al., 2019). However, to further dissect critical aspects of the microbial communities instigating inflammatory bone loss in the LIP model, it is crucial to better understand whether there is a conserved microbiome signature underlying inflammatory bone loss or perhaps there are different kinds of dysbiotic communities able to exacerbate inflammatory responses and trigger bone loss in this setting.

Similar to clinical human microbiome studies, the direct comparison of the microbiome profiles during LIP across studies is often very challenging, mainly due to significant dissimilarities in bioinformatic pipelines and databases utilized for analyses and taxonomic identification of 16S rDNA gene-based datasets, which have a known influence on the microbial signatures observed in these types of analyses (Abellan-Schneyder et al., 2021). In the present study, attempting to overcome these limitations, we conducted a reanalysis of 16S rDNA gene datasets from several published studies utilizing the LIP model. Then, these datasets were unified according to the hypervariable region of the 16S rDNA gene utilized for microbiome characterization (V4 or V1-V3) and subjected to the same bioinformatic preprocessing and reclassification, allowing for a direct comparison among studies. We analyzed microbial richness and diversity across studies and compared their microbial structure and relative abundance, focusing on taxonomic assignments with relevant databases. We believe this reanalysis provides an integrated vision of microbial dysbiosis during LIP and might serve as a valuable resource to further interrogate host–microbial interactions during periodontitis.

2 | MATERIALS AND METHODS

2.1 | Study selection and obtaining the sequencing datasets

We screened the current literature that analyzed the murine oral microbiome by 16S rDNA gene sequencing and selected studies that employed the ligature-induced periodontitis model. From the initially chosen studies, we kept those that performed the LIP model in non-genetically modified mouse strains, housed animals under specific pathogen-free conditions, did not test special diets, and that used the ligature as a microbial sample. Then, we finally selected nine studies; seven of them utilized primers amplifying the V4 hypervariable region of the 16S rRNA gene; one study focused on the V1-V2 hypervariable regions, and the other focused on the V1-V3 hypervariable regions (Table 1). Some of these studies had their raw datasets publicly available in different databases, such as the National Center Biotechnology Information (NCBI) and European Nucleotide Archive. When studies did not have their sequencing data publicly available, we requested it directly from the authors.

2.2 | Bioinformatic reprocessing of sequencing reads

Sequencing data from the nine studies available were separated and grouped for analysis into two sets according to the hypervariable regions of the 16S rDNA gene analyzed: V4 and V1-V3. We preferred to keep these two separate datasets (V4 and V1-V3), as it is well recognized that the hypervariable region of the 16S rDNA gene can influence microbial composition (Abellan-Schneyder et al., 2021). Sequencing reads were processed using mothur (Schloss et al., 2009) following a standard pipeline. Reads were quality filtered, assembled into contigs (if necessary), and filtered by size, keeping those of 200–520 bp in length in both groups. Reads were aligned to the 16S rRNA SILVA database (release 132) (Quast et al., 2013), and chimeric sequences were removed using VSEARCH (Rognes et al., 2016). Sequences were classified using the Ribosomal Database Project (RDP) classifier trainset v.18 (Wang et al., 2007), as implemented in mothur, with a cutoff = 80, followed by removal of all sequences mapping to chloroplasts, mitochondria, unknown, archaea, and eukaryota lineages. We defined

TABLE 1 Summary of all studies included in this reanalysis

Study (reference)	Number of samples	Study design	Mouse strain	Location of animal facility	Mouse vendor	DNA extraction method	Primers and 16S ribosomal RNA gene region sequenced	Platform used for sequencing
Dutzan et al. (2018)	10	Control and LIP microbiome samples at day 5 after LIP induction	C57BL/6	National Institute of Dental and Craniofacial Research	Jackson Laboratories	Modified version of DNeasy Blood and Tissue kit (Qiagen) that includes a chemical/enzymatic lysis step	515F–806R (V4)	Illumina MiSeq
Johnstone et al. (2021)	8	LIP microbiome samples at day 5 after LIP induction	C57BL/6	University of Minnesota	Jackson Laboratories	Enzyme digestion (lysozyme and mutanolysin) (SigmaAldrich) followed by bead-based isolation using the DNeasy Powerlyzer Powersoil kit (Qiagen)	Primers targeting V4 region (unspecified)	Illumina MiSeq
Kitamoto et al. (2020)	20	Control and LIP microbiome samples at days 3, 7, 10, and 14 after LIP induction	C57BL/6J	University of Minnesota	Jackson Laboratories	Modified protocol of the DNeasy Blood & Tissue Kit (Qiagen)	Primers targeting V4 region (unspecified)	Illumina MiSeq
Kittaka et al. (2019)	6	LIP microbiome samples at day 5 after LIP induction	C57BL/6	University of Missouri-Kansas City and Indiana University	Jackson Laboratories	Meta-G-Nome DNA Isolation Kit (Epicentre)	Primers targeting V4 region (unspecified)	Illumina MiSeq
Kittaka et al. (2020)	6	LIP microbiome samples at day 5 after LIP induction	C57BL/6J	University of Missouri-Kansas City and Indiana University	Jackson Laboratories	Meta-G-Nome DNA Isolation Kit (Epicentre)	Primers targeting V4 region (unspecified)	Illumina MiSeq

(Continues)

TABLE 1 (Continued)

Study (reference)	Number of samples	Study design	Mouse strain	Location of animal facility	Mouse vendor	DNA extraction method	Primers and 16S ribosomal RNA gene region sequenced	Platform used for sequencing
Tsukasaki et al. (2018)	18	Control (no bacteria detected) and LIP microbiome samples at days 3, 5, 7, 10, and 14 after LIP induction	C57BL/6J	University of Tokyo	Jackson Laboratories	NucleoSpin Tissue Kit (Takara)	515F–806R (V4)	Illumina MiSeq
Williams et al. (2020)	8	LIP microbiome samples at day 21 after LIP induction	C57BL/6	University of California, Los Angeles	CLEA Japan	DNeasy PowerSoil Kit (Qiagen)	515F–806R (V4)	Illumina MiSeq
Hoare et al. (2021)	5	LIP microbiome samples at day 5 after LIP induction	C57BL/6J	University of Pennsylvania	Jackson Laboratories	Lysozyme and proteinase K treatment and a DNeasy Blood and Tissue kit (Qiagen)	8F–361R (V1-V2)	Illumina MiSeq
Zheng et al. (2019)	10	LIP microbiome samples at day 7 after LIP induction	C57BL/6J	Monell Chemical Senses Center	Monell Chemical Senses Center	PureLink Microbiome DNA Purification Kit (Thermo Fisher Scientific)	27F–533R (V1-V3)	Illumina MiSeq

Abbreviation: LIP, ligature-induced periodontitis.

operational taxonomic units (OTUs) at 97% similarity and classified them up to the genus level when possible. Additionally, we further informed our taxonomical classification down to the species level by blasting the reference sequence of the OTUs against the NCBI 16S rRNA database (accessed in March 2022) using BLAST, and the top match with at least 97% similarity and coverage reported in parenthesis as part of the OTU name, as previously described (Abusleme et al., 2017, 2020; Dutzan et al., 2017). When a representative sequence matched multiple species, we selected the most likely oral species based on the literature (when possible). Our species level classification is reported in parentheses because it is an approximation and is not definitive. To explore other relevant databases for taxonomic classification, we also employed the Mouse Oral Microbiome Database (MOMD) (Joseph et al., 2021), a publicly available curated mouse oral microbiome database.

2.3 | Microbiome data analysis, statistics, and visualization

For the analysis of alpha-diversity, we used the number of observed OTUs as a richness estimator and the nonparametric version of the Shannon index and inverse Simpson index as diversity indexes, which were calculated in mothur. Principal coordinate analyses (PCoAs) of community structure were generated using mothur based on Yue-Clayton theta distances (θYC). Analysis of molecular variance was utilized to test for differences in community structure, as implemented in mothur. Differences in relative abundance between experimental time-points were evaluated using LEfSe (Segata et al., 2011), considering 0.01 as the α value for statistical testing.

All graphs were generated using R (version 4.1.2, https://www.r-project.org) and RStudio (Build 382, http://www.rstudio.com/). For data visualization, the R packages "ggplot2," version 3.3.5 (http://ggplot2.org), "reshape" version 0.8.8 (http://had.co.nz/reshape/), "ggh4x," version 0.2.1 (https://github.com/teunbrand/ggh4x), and "RColorBrewer" version 1.1-2 (https://CRAN.R-project.org/package = RColorBrewer) were used. For the statistical analyses of alpha-diversity estimates between the same experimental time points, we utilized the Kruskal–Wallis test and Dunn's multiple comparisons. These analyses were generated using GraphPad Prism 9 (GraphPad Software, San Diego, California, USA).

3 | RESULTS

3.1 | Selecting and merging the LIP microbiome datasets

To evaluate oral microbiome profiles associated with dysbiosis in the periodontal environment, we combined and reanalyzed the sequencing data (obtained by high-throughput 16S rDNA gene sequencing) from nine studies performing experimental periodontitis employing the LIP model. A total of 91 microbial samples were included in this reanalysis. Seven of them used primers targeting the V4 hypervariable region of the 16S rRNA gene (Dutzan et al., 2018; Johnstone et al., 2021; Kitamoto et al., 2020; Kittaka et al., 2020, 2019; Tsukasaki et al., 2018; Williams et al., 2020) and were merged for microbiome reanalyses. Additionally, two studies focused on the first hypervariable regions of the 16S rRNA gene; one targeted the V1-V2 regions (Hoare et al., 2021) and the other targeted the V1-V3 regions (Zheng et al., 2019). The sequencing data from both studies were merged for reprocessing. A summary of all studies included in this reanalysis is reviewed in Table 1. The microbiome analyses across studies presented important differences in their experimental design, as some collected samples ranging from days 0 (control) to 21, with only two studies including control or baseline samples (Table 1) (Dutzan et al., 2018; Kitamoto et al., 2020). Regarding the animals in each study, the C57BL7/6 mouse strain is utilized across all studies, and The Jackson Laboratories is the source for most studies (seven out of nine). All animal facilities where the animals were housed were different among studies, except for both studies authored by Kittaka et al. (2020, 2019). The DNA extraction method also differed in the majority of studies, but the most common method utilized was the DNeasy Blood & Tissue Kit (Qiagen) in five studies (Dutzan et al., 2018; Hoare et al., 2021; Johnstone et al., 2021; Kitamoto et al., 2020; Williams et al., 2020). Primer sequences and the exact location they span within the 16S rDNA gene were unspecified for four studies targeting the V4 region (Johnstone et al., 2021; Kitamoto et al., 2020; Kittaka et al., 2020, 2019), and the other three studies amplified the V4 region between positions 515F and 806R (Dutzan et al., 2018; Tsukasaki et al., 2018; Williams et al., 2020). For both studies targeting the first hypervariable regions of the 16S rDNA gene, the primer sets were provided. All the studies employed Illumina MiSeq as a platform for sequencing.

3.2 | Comparable microbial richness and diversity across studies and time points

First, we analyzed alpha-diversity measures across all studies, performing direct statistical comparisons only among studies presenting microbiome data at the same experimental time points defined as days after ligature placement.

For microbial richness within studies that analyzed the V4 hypervariable region, all samples displayed similar richness (depicted as the number of observed OTUs), except for the study by Kitamoto et al. (2020), in which microbial communities displayed a significantly higher richness at baseline (compared to controls from Dutzan et al.) and at days 3 and 7 after ligature placement when compared to microbial communities belonging to the Tsukasaki study (Tsukasaki et al., 2018) (Figure 1a).

Interestingly, on day 5 after ligature placement, which was the time point most commonly analyzed across all studies (five out of seven), all studies exhibited comparable microbiome richness, and there were no significant differences observed (Figure 1a).

In the studies analyzing the V1-V3 region, microbial richness was similar to that described for the studies based on the V4 region at both

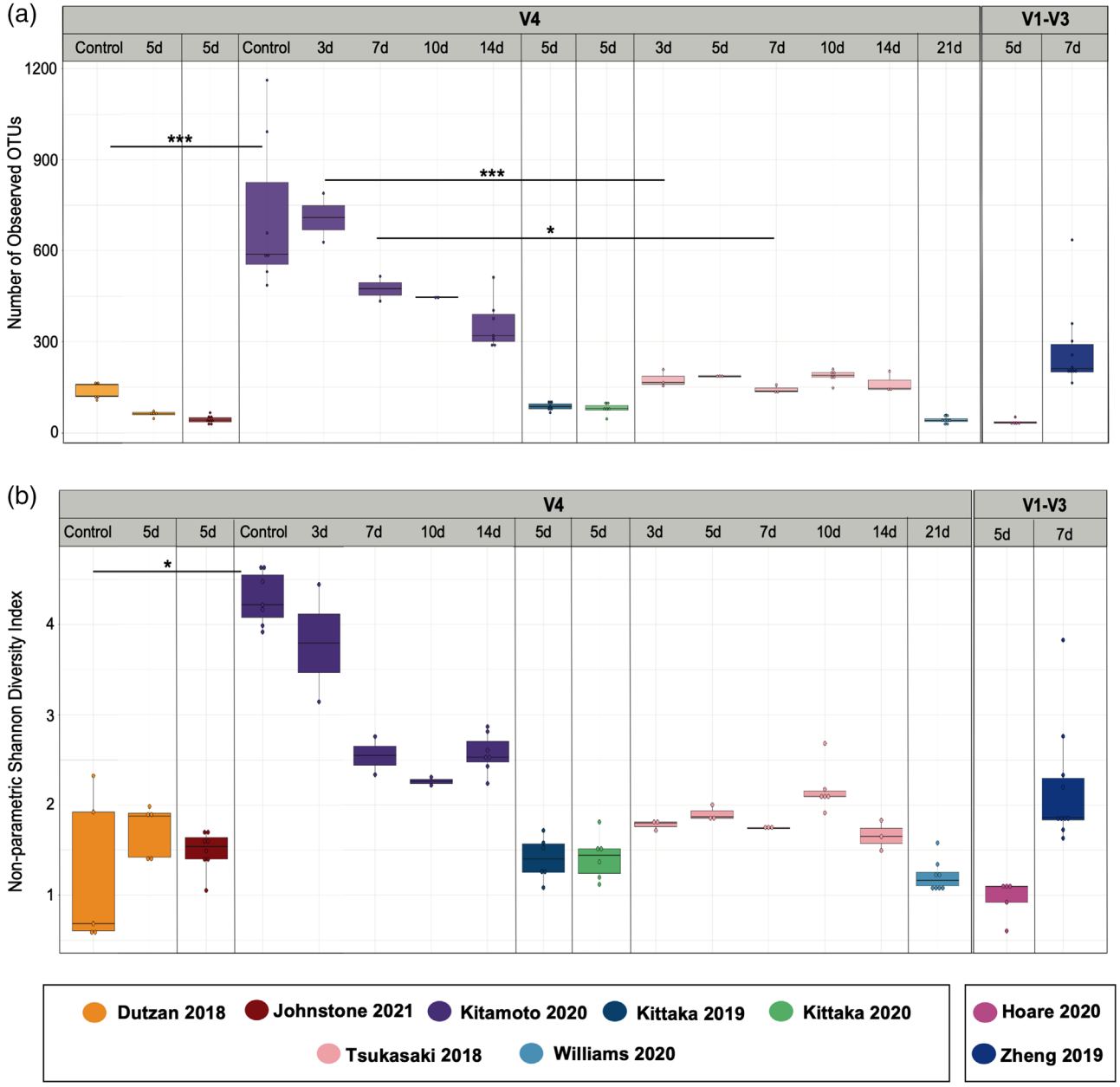

FIGURE 1 Alpha-diversity estimates for ligature-induced periodontitis (LIP)-associated microbial communities across studies and time points. (a) Number of bacterial species observed. Data were analyzed using the Kruskal–Wallis test and Dunn's multiple comparisons test for V4 reads, and these comparisons were only made between the same experimental time points. $^{*}p < 0.05$, $^{***}p < 0.001$. (b) Nonparametric Shannon diversity index. Data were analyzed using the Kruskal–Wallis test and Dunn's multiple comparisons test for V4 reads, and these comparisons were only made between the same experimental time points. $^{*}p < 0.05$

time points analyzed (5 and 7 days after ligature placement), as shown in Figure 1a.

In terms of microbial diversity (Figure 1b, Figure S1) , similar results to those of microbial richness were found. The Shannon and inverse Simpson diversity indexes did not reveal significant differences among studies except for Kitamoto et al. (2020), which displayed the highest diversity in their control samples, and this difference was significant when compared to control samples from Dutzan et al. (2018).

3.3 | Changes in community structure are influenced by periodontitis induction and study of origin

To evaluate the differences in global community structure among microbiome communities and thereby explore the relationships among datasets, PCoAs were performed (Figure 2a,b). These data showed that the study from which samples originated is a significant determinant of community structure ($p < 0.001$, Table S1), and this was true for

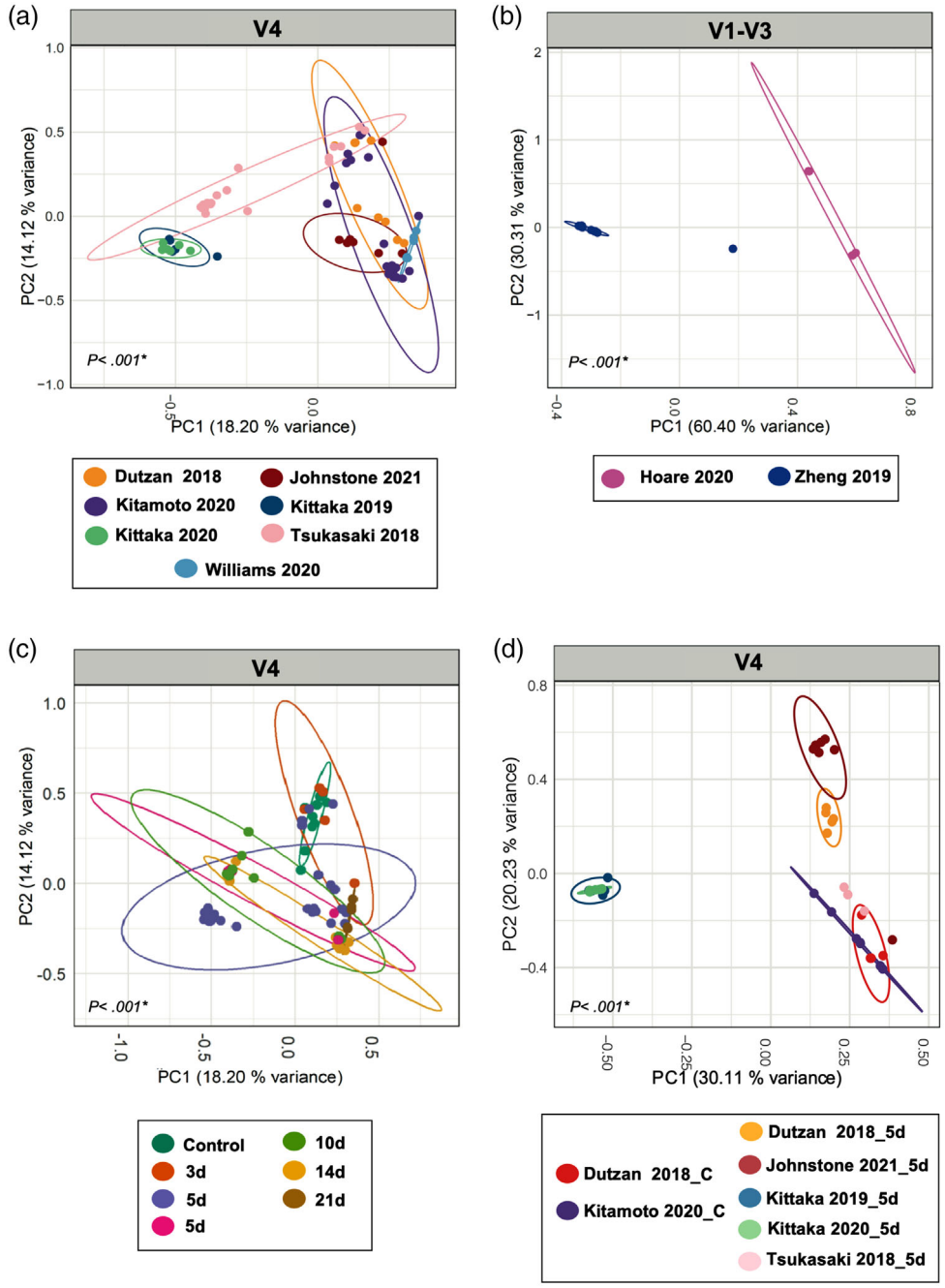

FIGURE 2 Beta-diversity estimates for microbial communities from different studies and time points. Principal coordinate analysis (PCoA) plots were constructed based on the ThetaYC distance, a measure of community structure. PCoA plots show clustering of microbial communities according to the study from which samples were obtained for the V4 group (a), V1-V3 group (b), according to the day from which samples were obtained for the V4 group (c), and for a selection of samples that were obtained for time-point control and day 5 in the V4 group (d). Data clouds are shown with 95% confidence ellipses. Significance ($p < 0.001$) of separation of data clouds was analyzed using analysis of molecular variance (AMOVA).

both the V4 and V1-V3 datasets. When comparing the similarity in microbiome structure among the samples by experimental time point in the V4 group (Figure 2c, Table S2), we also observed a significant separation of data clouds according to days after ligature placement ($p < 0.001$, Table S2). Interestingly, control samples were grouped as a distinct cluster of microbial samples, and there was a significant microbial shift of microbial structure from baseline to after periodontitis induction at all time points compared (Figure 2c–d, Tables S2 and S3).

Since day 5 after ligature placement was the time point most frequently included across the V4 studies (five of them), we decided to compare microbial structure among all microbial communities collected at this time point compared to controls (Figure 2d and Table S3). Despite homogenizing the day of sample collection, we still observed significant clustering according to the study of origin, reinforcing our previous findings. We also analyzed the differences in global community structure among microbiome communities selected from the three studies

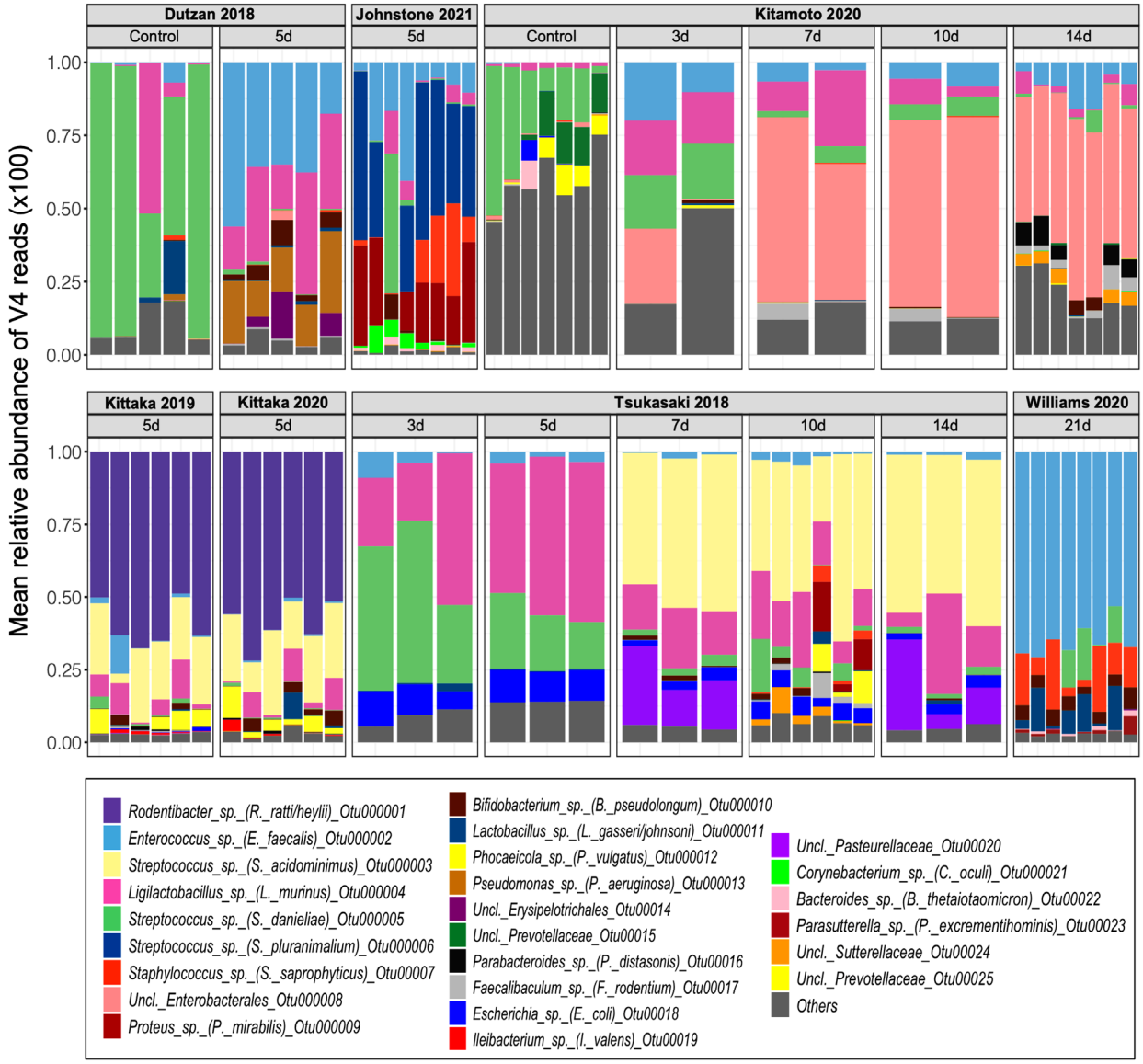

FIGURE 3 Overview of the most abundant bacterial operational taxonomic units (OTUs) in the ligature-induced periodontitis (LIP) microbiome of studies utilizing the V4 hypervariable region of the 16S rRNA gene. Relative abundance plot showing OTUs across communities from studies targeting the V4 region, separated by experimental time-point (in days after LIP induction). Species-level taxonomy is reported in parentheses when >97% similarity was achieved in National Center for Biotechnology Information (NCBI) BLAST. Each bar represents one sample.

performing longitudinal sampling (Dutzan et al., 2018; Kitamoto et al., 2020; Tsukasaki et al., 2018). We observed that control samples from Dutzan et al. (Figure S2a) and Kitamoto et al. (Figure S2b) and samples for days 3 and 5 (which were taken as "control samples," Figure S2c) in Tsukasaki et al. were all grouped into a distinct cluster of microbial samples, and then there was a significant microbial shift of microbial structure from baseline to after periodontitis induction (Figure S2a–c).

3.4 | Diverse microbiome profiles feature conserved microbial signatures across studies

Next, we sought to analyze the relative abundance of the most dominant taxa in each study, and marked differences in microbial profiles among studies emerged, again reinforcing the influence of the study of origin on microbial composition (Figures 3 and 4). Interestingly, the microbial profile observed in those studies that performed longitudinal sampling (Dutzan et al., 2018; Kitamoto et al., 2020; Tsukasaki et al., 2018) depicts a clear microbial transition in the relative abundance of bacterial taxa as days progress and dysbiosis ensues.

Despite the differences mentioned across studies, abundant and shared genera, such as *Streptococcus* and *Enterococcus*, were present in all periodontal microbial communities. For instance, an OTU identified as *Streptococcus* sp. (*Streptococcus danieliae*) constitutes a major proportion of relative abundance in control samples from Dutzan et al. (2018), Kitamoto et al. (2020), and day 3 samples from Tsukasaki et al. (2018), being significantly overrepresented when compared to LIP samples and decreasing as the days go by and dysbiosis evolves (Figure 3).

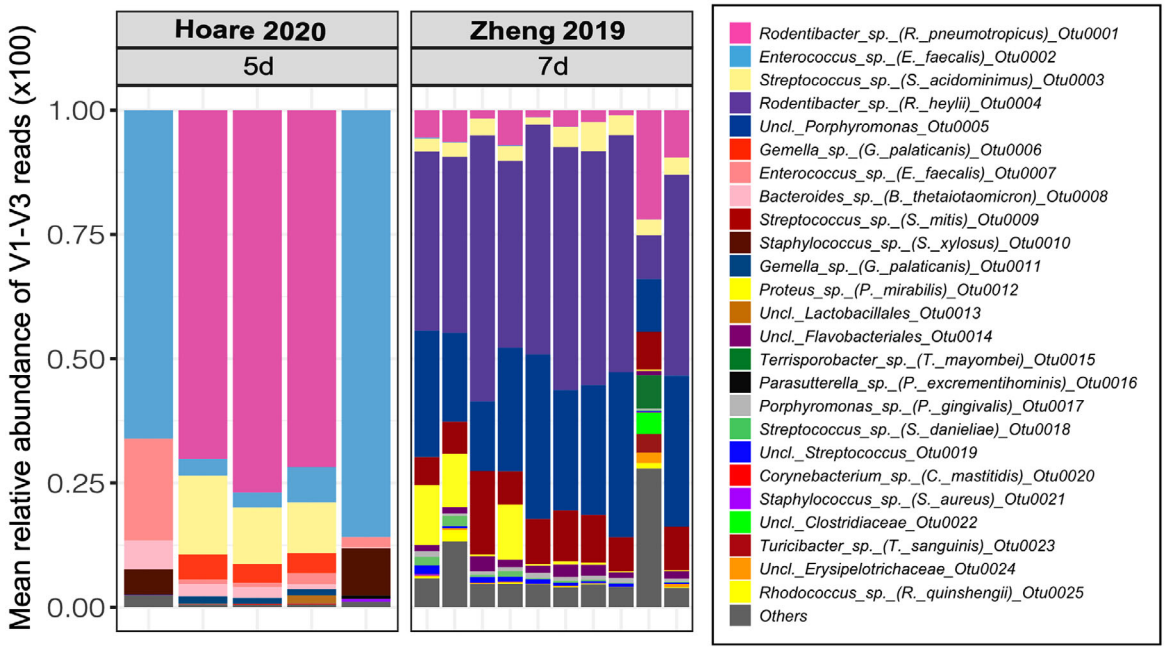

FIGURE 4 Overview of the most abundant bacterial operational taxonomic units (OTUs) in the ligature-induced periodontitis (LIP) microbiome of studies utilizing the V1-V3 hypervariable region of the 16S rRNA gene. Relative abundance plot showing OTUs across communities from studies targeting the V1-V3 regions, separated by experimental time point (in days after LIP induction). Species-level taxonomy is reported in parentheses when >97% similarity was achieved in National Center for Biotechnology Information (NCBI) BLAST. Each bar represents one sample.

Additionally, another conserved microbial signature between control samples was a consistent representation of OTUs belonging to the phyla *Firmicutes* and *Bacteroidetes* (Figure S3). An OTU affiliated with *Enterococcus* sp. (*Enterococcus faecalis*) showed the highest proportion in Williams et al. (2020) 21 days after LIP and in Dutzan et al. (2018) 5 days after LIP, and in the latter study, it was significantly increased from control to day 5 after ligature placement. Another shared bacterial taxon across studies was an OTU identified as *Ligalactobacillus* sp. (*Ligalactobacillus murinus*), which was present in all microbiome samples except for those belonging to Williams et al. (2020). Another OTU affiliated with a *Streptococcus* sp. (*Streptococcus acidominimus*) was mainly present in the study of Tsukasaki et al. (2018), increasing its relative abundance starting from day 7 until day 14 after ligature placement, and predominated at all later time points. Interestingly, this OTU identified as *Streptococcus* sp. (*S. acidominimus*) was also detected in both studies by Kittaka et al. (2020, 2019), being the second most abundant bacterial member of these communities, and was also detected in the V1-V3 studies of Hoare et al. (2021) and Zheng et al. (2019) (Figure 4), albeit at much lower abundance. The last dominant community member across studies was an OTU identified as *Rodentibacter* sp. (*Rodentibacter ratii/heylii*), which formerly belonged to the genus *Pasteurella*, predominated in the microbial communities of both studies of Kittaka et al. (2020, 2019) and Zheng et al. (2019) (Figures 3 and 4).

We also aimed to complement the taxonomic identities obtained in our datasets by utilizing a recently published and manually curated MOMD (Joseph et al., 2021) as an alternative to the RDP database (Wang et al., 2007). The RDP database was used in this study in conjunction with NCBI, the nucleotide database as previously described (Abusleme et al., 2020; Dutzan et al., 2017). As shown in Figure S4, the taxonomic resolution utilizing MOMD for the V4 region studies yields several OTUs as unclassified or at a higher taxonomic level than the taxonomic information obtained with the combination of RDP/NCBI nucleotide databases for the same dataset. However, there was an improvement in taxonomic assignment to OTUs for the V1-V3 studies, reaching genus-level identifications and species-level suggestions more often than with RDP/NCBI.

3.5 | The relationship of microbiome profiles during LIP with periodontitis progression

Importantly, we document that different profiles of dysbiotic microbial communities across studies are linked with periodontitis progression, traditionally measured as alveolar bone loss. We observed that in the three studies that included longitudinal sampling (Dutzan et al., 2018; Kitamoto et al., 2020; Tsukasaki et al., 2018), the microbial accumulation elicited by the ligature induced significant alveolar bone loss of 0.4 mm after 5 days of placement (Dutzan et al., 2018) and 1.5 mm after the same 5 days of LIP induction and nearly 3 mm at 14 days after ligature placement (Tsukasaki et al., 2018). Additionally, the study by Kitamoto et al. (2020) also reports visible bone loss at day 14 after ligature placement, albeit without providing specific values. Taken together, these observations suggest that different kinds of dysbiosis induced by the LIP model in the periodontal environment are able to trigger alveolar bone loss in a comparable manner; despite

exhibiting some variations in magnitude, bone resorption is significant when compared with the baseline bone levels within each study.

3.6 | Distinct overrepresented bacterial taxa characterize periodontal health and LIP-associated communities

To better define differentially represented taxa in control samples and LIP-associated communities, we further analyzed the three studies that included a longitudinal sampling strategy (Dutzan et al., 2018; Kitamoto et al., 2020; Tsukasaki et al., 2018). To this end, we performed statistical analyses to define which taxa, at the OTU, genus and phylum levels, were significantly associated with each condition (Figures 5–7 and Figures S5–S7). As representative of periodontal health, we included the control samples for both Dutzan et al. (2018) and Kitamoto et al. (2020) and considered the samples from days 3 and 5 as controls for the study of Tsukasaki et al. (2018). In these control samples, *Streptococcus* sp. (*S. danieliae*) was the top differentially represented OTU, strongly associated with periodontal health (Figures 5–7). Additionally, other OTUs belonging to the *Muribaculaceae* family were consistently overrepresented in health as well across the three studies (Figures 5–7).

In LIP-associated samples, *Enterococcus* sp. (*E. faecalis*) was the top differentially represented OTU in the study of Dutzan et al. (2018) and the second differentially represented OTU in the study of Kitamoto et al. (2020) (Figures 5 and 6). For the study of Tsukasaki et al. (2018), *Streptococcus* sp. (*S. acidominimus*) was the top overrepresented community OTU member (Figure 7). Interestingly, *Faecalibaculum* sp. (*Faecalibaculum rodentium*) was differentially represented across the three studies in periodontitis samples (Figures 5–7).

At the genus level, *Streptococcus* was the most abundant taxa in control samples for Dutzan and Kitamoto (Dutzan et al., 2018; Kitamoto et al., 2020) (Figures S5a and S6a, respectively), and for days 3/5 for the study of Tsukasaki et al. (2018), *Ligalactobacillus* was the top differentially represented genus (Figure S7a). For LIP-associated taxa, the top overrepresented genus was *Enterococcus* for the study of Dutzan et al. (2018), *Klebsiella* for the study of Kitamoto et al. (2020), and *Duncaniella* for the study of Tsukasaki et al. (2018) (Figures S5a, S6a, and S7a).

At the phylum level, the top differentially represented phylum in health-associated communities was *Firmicutes* for the studies of Dutzan et al. (2018) and Kitamoto et al. (2020) (Figures S5b and S6b), and no taxa were significantly overrepresented in the study of Tsukasaki et al. (2018) (Figure S7b). For the LIP-associated communities, the differentially represented phyla were *Proteobacteria* and *Actinobacteria* for the microbial communities from the studies of Dutzan et al. (2018) and Kitamoto et al. (2020) (Figures S5b and S6b). *Actinobacteria* was also overrepresented in the microbiome samples of the study of Tsukasaki et al. (2018) along with *Verrucomicrobia* (Figure S7b).

Finally, we provide an overview of the differentially represented taxa associated with periodontal health and the LIP model in the murine setting. To accomplish this, we analyzed the bacterial OTUs enriched in healthy or LIP-associated communities obtained from differential abundance analyses and established specific significance cutoffs for OTUs, which should have an LDA value >3 and were detected in at least two studies, to ensure their strong association with each periodontal condition. We found that an OTU identified as *Streptococcus* sp. (*S. danieliae*) and an OTU belonging to the *Muribaculaceae* family defined periodontal health, while OTUs affiliated with *Faecalibaculum* sp. (*F. rodentium*), *Enterococcus* sp. (*E. faecalis*), *Bifidobacterium* sp. (*B. pseudolongum*), and *Adlercreutzia* sp. were the most abundant and represented during LIP across studies (Figure 8).

4 | DISCUSSION

Our study reveals important insights regarding the microbial dysbiosis underlying the LIP model across several studies. In an attempt to unify and homogenize the microbiome analyses available to date during LIP, we combined and reanalyzed the murine oral microbiome data from nine comparable studies employing this animal model with standardized parameters (Dutzan et al., 2018; Hoare et al., 2021; Johnstone et al., 2021; Kitamoto et al., 2020; Kittaka et al., 2020, 2019; Tsukasaki et al., 2018; Williams et al., 2020; Zheng et al., 2019).

The advent of next-generation sequencing techniques for microbiome characterization and the widespread use of animal models to study periodontitis pathogenesis have allowed us to considerably expand our understanding of the role of microbial communities as instigators of alveolar bone loss. Among the strategies that have been utilized to induce experimental periodontitis in mice, the LIP method has become a widely adopted murine model, as it is capable of inducing alveolar bone loss within a few days, accompanied by a microbial shift that constitutes a significant driver for this process (Abe & Hajishengallis, 2013; Dutzan et al., 2018; Kitamoto et al., 2020; Tsukasaki et al., 2018). Hence, the LIP model is characterized by the establishment of microbial dysbiosis without further manipulation, providing a relevant experimental setting for the study of these communities in the context of our current understanding of the polymicrobial oral dysbiosis associated with periodontitis pathogenesis (Hajishengallis & Lamont, 2021). Therefore, in this study, we aimed to synthesize and reanalyze the microbiome signatures that characterize LIP. Nonetheless, we fully recognize several experimental differences among studies as an important limitation when comparing these data, influencing this current reanalysis.

We document that all studies presented some dissimilarities in their methodology, such as the different DNA extraction methods across studies (only five out of nine employed the same protocol), which is a known factor that might influence oral microbial profiles (Abusleme et al., 2014). On the other hand, all animals belonged to the same isogenic lineage (C57BL/6), but some of them were obtained from different vendors (Williams et al., 2020; Zheng et al., 2019). It has been previously shown that mice from different vendors exhibit distinct oral, gut, and fecal microbial communities (Abusleme et al., 2020; Dutzan et al., 2017; Ivanov et al., 2009; Rausch et al., 2016). The animal facility is also a critical factor that influences the composition

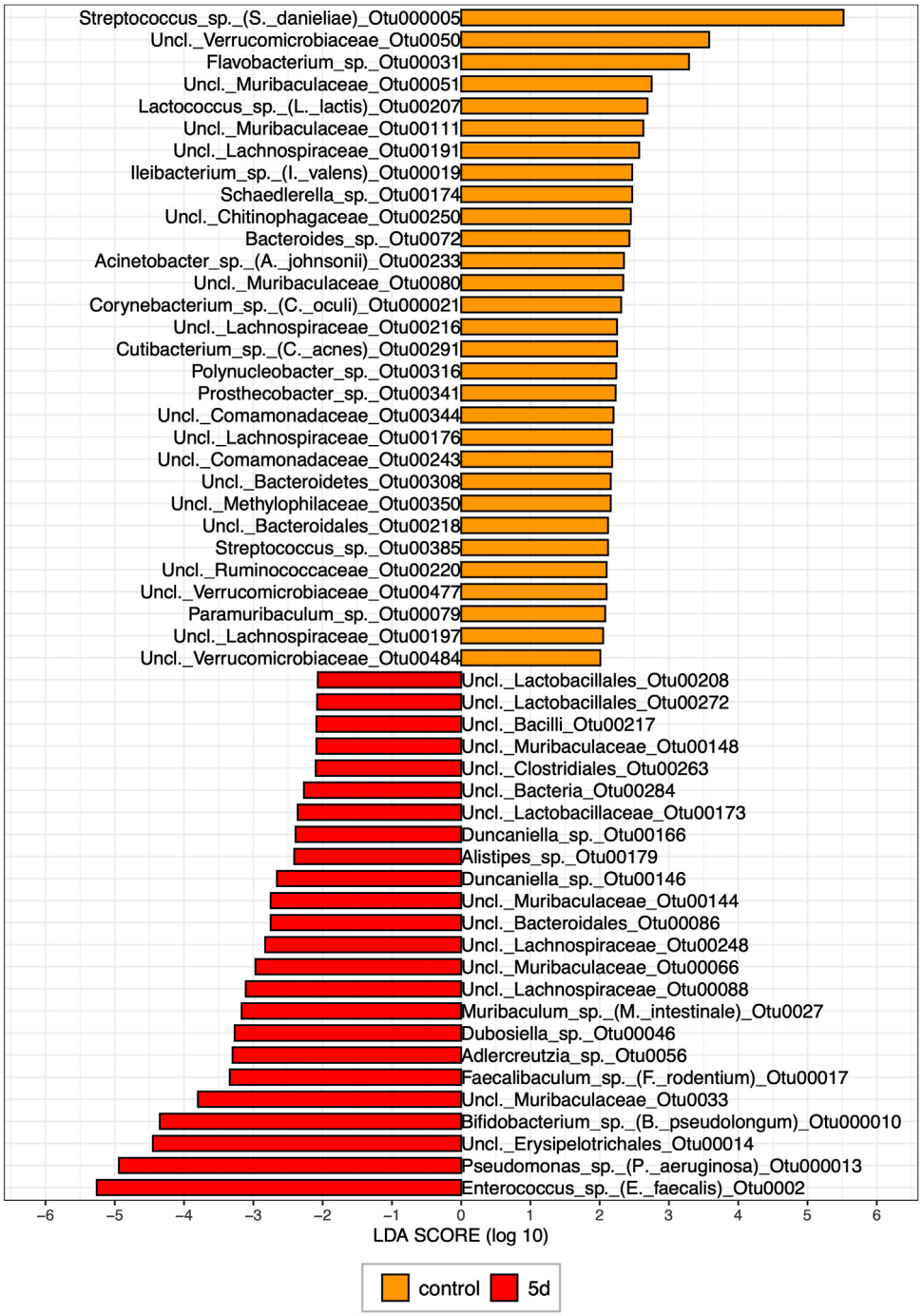

FIGURE 5 Differentially represented operational taxonomic units (OTUs) in ligature-induced periodontitis (LIP) and control samples from Dutzan et al. (2018). The graph shows taxa differentially represented according to LEfSe analyses comparing control and day 5 samples after LIP classified at the OTU/species level. Bars represent linear discriminant analysis (LDA) scores.

of the microbiome profile in mice, as it has been recently shown for gut microbial communities, which undergo microbial shifts while acclimating to a new vivarium regardless of the vendor of origin; however, there is an important fraction of shared OTUs that is still retained (Long et al., 2021). We recognize that there are several environmental aspects related to animal facility practices and inherent differences within each vivarium that can dramatically impact the overall microbiome of laboratory mice. For instance, extrinsic factors of the environment ranging from the flaking of the skin or dust particles coming from caretakers and scientists who constantly handle the mice to the pH of the water and the treatment and kind of food provided are key factors that might be constantly shaping microbial colonization in laboratory mice (Long et al., 2021; Rausch et al., 2016). These variables are likely affecting the early microbial assembly of the oral microbiome, ultimately influencing the microbial communities at the time of assessing microbial composition and structure (Abusleme et al., 2020).

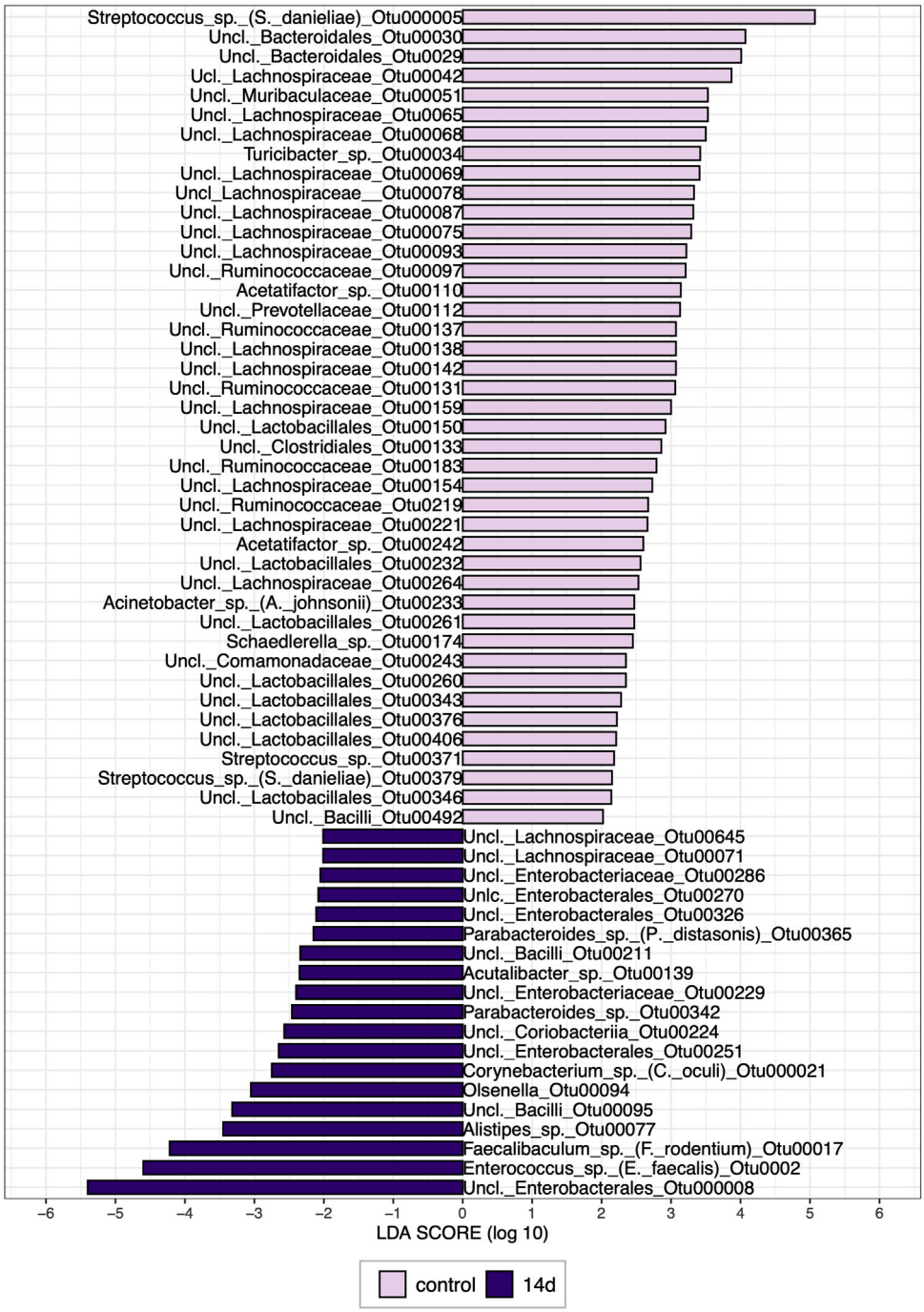

FIGURE 6 Differentially represented operational taxonomic units (OTUs) in ligature-induced periodontitis (LIP) and control samples from Kitamoto et al. (2020). The graph shows taxa differentially represented according to LEfSe analyses comparing control and day 14 samples after LIP, classified at the OTU/species level. Bars represent linear discriminant analysis (LDA) scores.

Our findings revealed similar richness and diversity across studies, as we observed that on day 5 after ligature placement, all studies that evaluated microbial communities at this time-point exhibited comparable microbiome richness and diversity (Dutzan et al., 2018; Kitamoto et al., 2020; Kittaka et al., 2020, 2019; Tsukasaki et al., 2018). The only exception was the study of Kitamoto et al. (2020), which exhibited increased richness and diversity compared with all other studies included at similar time points. This might be due to inherent experimental and/or methodological differences in that particular study (Kitamoto et al., 2020), as we can affirm that these differences were not related to a higher sequencing depth because libraries were normalized to the exact read count to obtain alpha-diversity estimates from all studies.

We found that community structure, independent of the 16S rDNA gene region analyzed, is largely defined by periodontitis induction and the study from which samples originated. These findings raise an

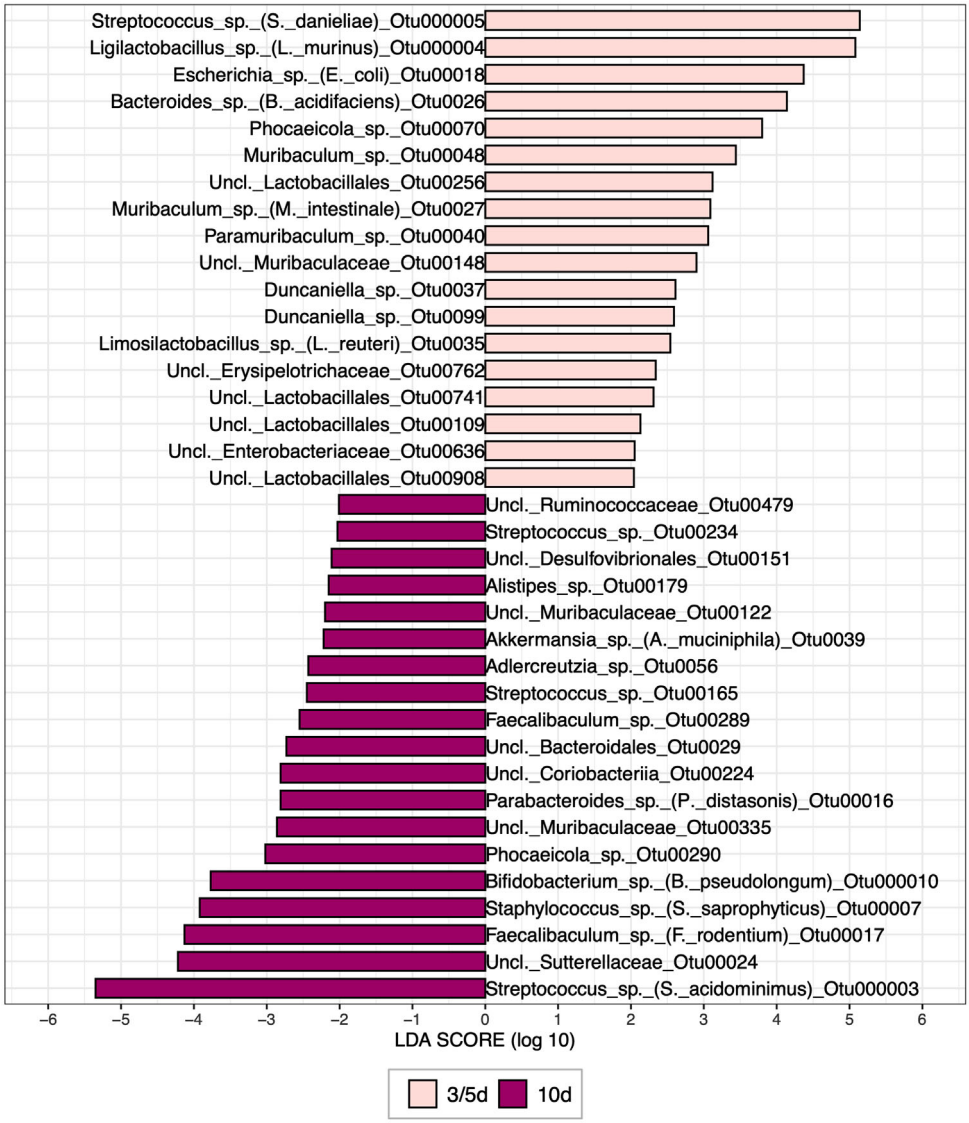

FIGURE 7 Differentially represented operational taxonomic units (OTUs) ligature-induced periodontitis (LIP) and control samples from Tsukasaki et al. (2018). The graph shows taxa differentially represented according to LEfSe analyses comparing day 3/5 (considered "controls") and day 10 samples after LIP, classified at the OTU/species level. Bars represent linear discriminant analysis (LDA) scores.

interesting aspect regarding the conserved ability of the LIP model to trigger shifts in periodontal microbial structure across studies, an aspect we could infer from the literature but, due to important differences in bioinformatic analyses, was difficult to ascertain and visualize. Relevant studies reanalyzing murine gut microbiome datasets have also described consistent microbial structure alterations in the setting of a known mouse model that induces obesity and metabolic alterations (the "high-fat diet" model) (Bisanz et al., 2019) and during aging (You et al., 2022). These meta-analyses have also revealed that each study has a marked influence on the microbial structure, but this did not seem to alter the reproducibility of the microbial alterations observed with the experimental model or variable of interest.

We observed a clear microbial shift in the relative abundance of bacterial taxa as days progressed in the studies that included longitudinal sampling (Dutzan et al., 2018; Kitamoto et al., 2020; Tsukasaki et al., 2018). The characterization of the microbial communities accumulating in the ligature has revealed that these communities undergo extensive changes in microbial structure and composition, leading to microbial dysbiosis. This process of microbial accumulation and marked shifts in community dynamics seem to recapitulate the microbial transition that occurs in humans from periodontal health to disease, albeit at a much faster pace and with different dominant taxa (Abusleme et al., 2021) (Hajishengallis & Lamont, 2021). Indeed, our findings revealed markedly different profiles of dysbiotic microbial communities across studies. We acknowledge that experimental aspects inherent to each study and interindividual sample variation may account in part for these distinct microbial signatures. However, different subgingival community types can also be recognized during human periodontitis (Beyer et al., 2018; Hong et al., 2015); hence, this microbiome variation associated with LIP may reflect that heterogeneity as well. On

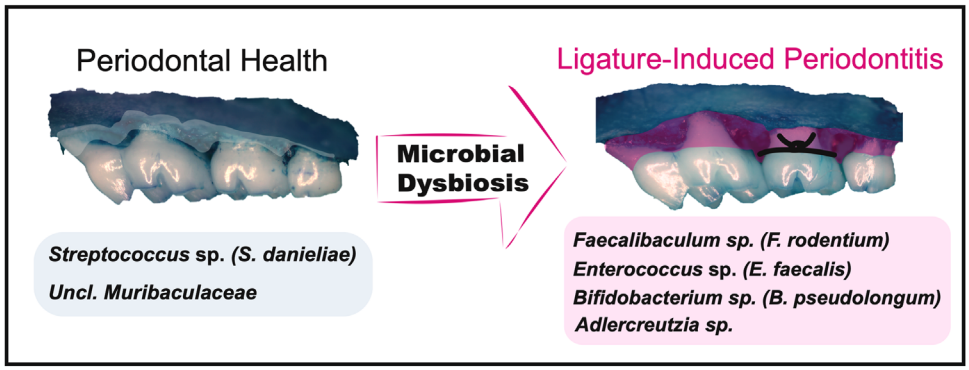

FIGURE 8 Summary of differentially represented operational taxonomic units (OTUs) in periodontal health and during ligature-induced periodontitis (LIP). The figure depicts OTUs that were significantly overrepresented in healthy individuals or LIPs across three studies with longitudinal sampling. OTUs depicted were selected based on linear discriminant analysis (LDA) values (higher than 3) and were detected in at least two out of the three studies included for these comparisons.

the other hand, even though in general microbial communities from all studies exhibit a conserved microbial signature upon LIP to a certain extent, there were some exceptions. For instance, the studies of Kittaka et al. (2019, 2020) clearly cluster away in terms of microbial structure from all studies and exhibit a unique microbial taxonomical profile, indicating that they are different from what is observed throughout the rest of the microbial communities upon LIP. A possible reason for this is the use of a different DNA isolation method than most studies or perhaps the performance of the primers utilized in this study, allowing the capture of slightly different microbial profiles.

Despite bacterial community variation across studies, we document conserved bacterial species taking part in ligature-associated microbial communities at baseline and during periodontitis induction. An OTU identified as *Streptococcus* sp. (*S. danieliae*) significantly dominates periodontal communities during health and was also consistently detected, albeit at much lower abundance, from microbiome samples after 5 or more days of ligation. This finding indicates that *Streptococcus* sp. (*S. danieliae*) may well be a core bacterial species of murine oral communities that particularly thrives during health, as has been consistently described in other studies (Abusleme et al., 2020; Benga et al., 2014; Hernandez-Arriaga et al., 2019; Joseph et al., 2021). Regarding the bacterial species that were abundant and prevalent in the LIP-associated community, an OTU affiliated with *Enterococcus* sp. (*E. faecalis*) was the most abundant across studies and differentially represented in longitudinal studies, followed by an OTU identified as *Ligalactobacillus* sp. (*L. murinus*). *Enterococcus* sp. (*E. faecalis*) seems to thrive in different settings of oral immune dysregulation in mice in addition to ligature-induced periodontitis, such as a model of candidiasis during corticoid-immunosuppression (Bertolini et al., 2021). *Ligalactobacillus* sp. (*L. murinus*) has been widely detected across studies assessing the mucosal and periodontitis-associated microbiome in mice (Abusleme et al., 2020; Dutzan et al., 2017; Payne et al., 2019). Other bacterial taxa frequently associated with LIP across studies were OTUs identified as *Streptococcus* sp. (*S. acidominimus*) and *Rodentibacter* sp. (*R. ratti/heylii*) microorganisms that have been described as commensals on mucosal surfaces (Benga et al., 2018). Last, OTUs affiliated with *Proteus* sp. (*Proteus mirabilis*) was also abundant and prevalent in the reanalyzed dataset of LIP samples. Interestingly, other members of the *Enterobacteriaceae* family (*Klebsiella* sp.) have been reported to dominate the communities associated with experimental periodontitis during LIP, promoting colitis and driving the differentiation of specific Th17 cells at the oral mucosa that can migrate to the gut (Kitamoto et al., 2020). However, the precise mechanisms by which the majority of the oral pathobionts flourishing in experimental periodontitis contribute to disease pathogenesis remain largely unexplored. Unraveling these mechanisms might shed light on important aspects related to host–microbial interactions during periodontitis.

In an effort to improve the taxonomic resolution in our reanalysis, we included the recently developed MOMD database (Joseph et al., 2021), which had a better performance with the V1-V3 datasets than V4. It has been recognized that the first 500 bp of the 16S rRNA gene (which spans the V1-V3 hypervariable regions) allows for improved taxonomic discrimination of human oral bacteria (Diaz et al., 2012). Our results suggest that this may also be the case for the murine oral microbiota, although future studies are required to investigate this possibility.

Taken together, this study offers a unified overview of microbial shifts associated with experimental periodontitis (LIP model) across different studies, obtained utilizing the same bioinformatic and taxonomic identification approaches, facilitating the analysis of the dysbiotic communities associated with periodontitis, providing new insights to expand the knowledge of host–microbial interactions at the periodontal interface.

ACKNOWLEDGMENTS

This study was funded by ANID, FONDECYT grants 11180505 (to Loreto Abusleme) and 11180389 (to Nicolas Dutzan), the Chilean government. Marion Arce is a recipient of scholarship ANID 21221003 from the Chilean Government.

CONFLICT OF INTEREST

The authors declare no conflict of interest.

DATA AVAILABILITY STATEMENT

The data that support the findings of this study are available from the corresponding author upon reasonable request.

ORCID

Marion Arce https://orcid.org/0000-0001-9841-9405
Natalia Endo https://orcid.org/0000-0002-9276-2234
Nicolas Dutzan https://orcid.org/0000-0001-8343-0214
Loreto Abusleme https://orcid.org/0000-0002-7210-1236

REFERENCES

Abe, T., & Hajishengallis, G. (2013). Optimization of the ligature-induced periodontitis model in mice. *Journal of Immunological Methods*, *394*(1–2), 49–54. https://doi.org/10.1016/j.jim.2013.05.002

Abellan-Schneyder, I., Matchado, M. S., Reitmeier, S., Sommer, A., Sewald, Z., Baumbach, J., List, M., & Neuhaus, K. (2021). Primer, pipelines, parameters: Issues in 16S rRNA gene sequencing. *mSphere*, *6*(1), e01202–20. https://doi.org/10.1128/mSphere.01202-20

Abusleme, L., Dupuy, A. K., Dutzan, N. S., Silva, N., Burleson, J. A., Strausbaugh, L. D., Gamonal, J., & Diaz, P. I. (2013). The subgingival microbiome in health and periodontitis and its relationship with community biomass and inflammation. *The ISME Journal*, *7*(5), 1016–1025. https://doi.org/10.1038/ismej.2012.174

Abusleme, L., Hoare, A., Hong, B. Y., & Diaz, P. I. (2021). Microbial signatures of health, gingivitis, and periodontitis. *Periodontology 2000*, *86*(1), 57–78. https://doi.org/10.1111/prd.12362

Abusleme, L., Hong, B. Y., Dupuy, A. K., Strausbaugh, L. D., & Diaz, P. I. (2014). Influence of DNA extraction on oral microbial profiles obtained via 16S rRNA gene sequencing. *Journal of Oral Microbiology*, *6*, 23990. https://doi.org/10.3402/jom.v6.23990

Abusleme, L., Hong, B. Y., Hoare, A., Konkel, J. E., Diaz, P. I., & Moutsopoulos, N. M. (2017). Oral microbiome characterization in murine models. *Bio Protocol*, *7*(24), e2655. https://doi.org/10.21769/BioProtoc.2655

Abusleme, L., O'Gorman, H., Dutzan, N., Greenwell-Wild, T., & Moutsopoulos, N. M. (2020). Establishment and stability of the murine oral microbiome. *Journal of Dental Research*, *99*(6), 721–729. https://doi.org/10.1177/0022034520915485

Bao, K., Li, X., Poveda, L., Qi, W., Selevsek, N., Gumus, P., Emingil, G., Grossmann, J., Diaz, P. I., Hajishengallis, G., Bostanci, N., & Belibasakis, G. N. (2020). Tissue in health and disease. *Frontiers in Cellular and Infection Microbiology*, *10*, 588155. https://doi.org/10.3389/fcimb.2020.588155

Benga, L., Benten, W. P., Engelhardt, E., Kohrer, K., Gougoula, C., & Sager, M. (2014). 16S ribosomal DNA sequence-based identification of bacteria in laboratory rodents: A practical approach in laboratory animal bacteriology diagnostics. *Laboratory Animals*, *48*(4), 305–312. https://doi.org/10.1177/0023677214538240

Benga, L., Sager, M., & Christensen, H. (2018). From the [Pasteurella] pneumotropica complex to *Rodentibacter* spp.: An update on [Pasteurella] pneumotropica. *Veterinary Microbiology*, *217*, 121–134. https://doi.org/10.1016/j.vetmic.2018.03.011

Bertolini, M., Vazquez Munoz, R., Archambault, L., Shah, S., Souza, J. G. S., Costa, R. C., Thompson, A., Zhou, Y., Sobue, T., & Dongari-Bagtzoglou, A. (2021). Mucosal bacteria modulate *Candida albicans* virulence in oropharyngeal candidiasis. *mBio*, *12*(4), e0193721. https://doi.org/10.1128/mBio.01937-21

Beyer, K., Zaura, E., Brandt, B. W., Buijs, M. J., Brun, J. G., Crielaard, W., & Bolstad, A. I. (2018). Subgingival microbiome of rheumatoid arthritis patients in relation to their disease status and periodontal health. *PLoS One*, *13*(9), e0202278. https://doi.org/10.1371/journal.pone.0202278

Bisanz, J. E., Upadhyay, V., Turnbaugh, J. A., Ly, K., & Turnbaugh, P. J. (2019). Meta-analysis reveals reproducible gut microbiome alterations in response to a high-fat diet. *Cell Host & Microbe*, *26*(2), 265–272.e264. https://doi.org/10.1016/j.chom.2019.06.013

Curtis, M. A., Diaz, P. I., & Van Dyke, T. E. (2020). The role of the microbiota in periodontal disease. *Periodontology 2000*, *83*(1), 14–25. https://doi.org/10.1111/prd.12296

Diaz, P. I., Dupuy, A. K., Abusleme, L., Reese, B., Obergfell, C., Choquette, L., Dongari-Bagtzoglou, A., Peterson, D. E., Terzi, E., & Strausbaugh, L. D. (2012). Using high throughput sequencing to explore the biodiversity in oral bacterial communities. *Molecular Oral Microbiology*, *27*(3), 182–201. https://doi.org/10.1111/j.2041-1014.2012.00642.x

Duran-Pinedo, A. E., Chen, T., Teles, R., Starr, J. R., Wang, X., Krishnan, K., & Frias-Lopez, J. (2014). Community-wide transcriptome of the oral microbiome in subjects with and without periodontitis. *The ISME Journal*, *8*(8), 1659–1672. https://doi.org/10.1038/ismej.2014.23

Dutzan, N., Abusleme, L., Bridgeman, H., Greenwell-Wild, T., Zangerle-Murray, T., Fife, M. E., Bouladoux, N., Linley, H., Brenchley, L., Wemyss, K., Calderon, G., Hong, B.-Y., Break, T. J., Bowdish, D. M. E., Lionakis, M. S., Jones, S. A., Trinchieri, G., Diaz, P. I., Belkaid, Y., … Moutsopoulos, N. M. (2017). On-going mechanical damage from mastication drives homeostatic Th17 cell responses at the oral barrier. *Immunity*, *46*(1), 133–147. https://doi.org/10.1016/j.immuni.2016.12.010

Dutzan, N., Kajikawa, T., Abusleme, L., Greenwell-Wild, T., Zuazo, C. E., Ikeuchi, T., Brenchley, L., Abe, T., Hurabielle, C., Martin, D., Morell, R. J., Freeman, A. F., Lazarevic, V., Trinchieri, G., Diaz, P. I., Holland, S. M., Belkaid, Y., Hajishengallis, G., & Moutsopoulos, N. M. (2018). A dysbiotic microbiome triggers TH17 cells to mediate oral mucosal immunopathology in mice and humans. *Science Translational Medicine*, *10*(463), eaat0797. https://doi.org/10.1126/scitranslmed.aat0797

Griffen, A. L., Beall, C. J., Campbell, J. H., Firestone, N. D., Kumar, P. S., Yang, Z. K., Podar, M., & Leys, E. J. (2012). Distinct and complex bacterial profiles in human periodontitis and health revealed by 16S pyrosequencing. *The ISME Journal*, *6*(6), 1176–1185. https://doi.org/10.1038/ismej.2011.191

Hajishengallis, G., & Lamont, R. J. (2021). Polymicrobial communities in periodontal disease: Their quasi-organismal nature and dialogue with the host. *Periodontology 2000*, *86*(1), 210–230. https://doi.org/10.1111/prd.12371

Hajishengallis, G., Lamont, R. J., & Graves, D. T. (2015). The enduring importance of animal models in understanding periodontal disease. *Virulence*, *6*(3), 229–235. https://doi.org/10.4161/21505594.2014.990806

Hernandez-Arriaga, A., Baumann, A., Witte, O. W., Frahm, C., Bergheim, I., & Camarinha-Silva, A. (2019). Changes in oral microbial ecology of C57BL/6 mice at different ages associated with sampling methodology. *Microorganisms*, *7*(9), 283. https://doi.org/10.3390/microorganisms7090283

Hoare, A., Wang, H., Meethil, A., Abusleme, L., Hong, B. Y., Moutsopoulos, N. M., Marsh, P. D., Hajishengallis, G., & Diaz, P. I. (2021). A cross-species interaction with a symbiotic commensal enables cell-density-dependent growth and in vivo virulence of an oral pathogen. *The ISME Journal*, *15*(5), 1490–1504. https://doi.org/10.1038/s41396-020-00865-y

Hong, B. Y., Furtado Araujo, M. V., Strausbaugh, L. D., Terzi, E., Ioannidou, E., & Diaz, P. I. (2015). Microbiome profiles in periodontitis in relation to host and disease characteristics. *PLoS One*, *10*(5), e0127077. https://doi.org/10.1371/journal.pone.0127077

Ivanov, I. I., Atarashi, K., Manel, N., Brodie, E. L., Shima, T., Karaoz, U., Wei, D., Goldfarb, K. C., Santee, C. A., Lynch, S. V., Tanoue, T., Imaoka, A., Itoh, K., Takeda, K., Umesaki, Y., Honda, K., & Littman, D. R. (2009). Induction of intestinal Th17 cells by segmented filamentous bacteria. *Cell*, *139*(3), 485–498. https://doi.org/10.1016/j.cell.2009.09.033

Johnstone, K. F., Wei, Y., Bittner-Eddy, P. D., Vreeman, G. W., Stone, I. A., Clayton, J. B., Reilly, C. S., Walbon, T. B., Wright, E. N., Hoops, S. L., & Boyle, W. S., Costalonga, M., & Herzberg, M. C. (2021). Calprotectin (S100A8/A9) is an innate immune effector in experimental periodontitis. *Infection and Immunity*, *89*(10), e0012221. https://doi.org/10.1128/IAI.00122-21

Joseph, S., Aduse-Opoku, J., Hashim, A., Hanski, E., Streich, R., Knowles, S. C. L., Pedersen, A. B., Wade, W. G., & Curtis, M. A. (2021). A 16S rRNA gene and draft genome database for the murine oral bacterial community. *mSystems*, *6*(1), e01222–20. https://doi.org/10.1128/mSystems.01222-20

Kitamoto, S., Nagao-Kitamoto, H., Jiao, Y., Gillilland, M. G., Hayashi, A., Imai, J., Sugihara, K., Miyoshi, M., Brazil, J. C., Kuffa, P., Hill, B. D., Rizvi, S. M., Wen, F., Bishu, S., Inohara, N., Eaton, K. A., Nusrat, A., Lei, Y. u. L., Giannobile, W. V., & Kamada, N. (2020). The intermucosal connection between the mouth and gut in commensal pathobiont-driven colitis. *Cell*, *182*(2), 447–462.e414. https://doi.org/10.1016/j.cell.2020.05.048

Kittaka, M., Yoshimoto, T., Schlosser, C., Kajiya, M., Kurihara, H., Reichenberger, E. J., & Ueki, Y. (2020). Microbe-dependent exacerbated alveolar bone destruction in heterozygous cherubism mice. *JBMR Plus*, *4*(6), e10352. https://doi.org/10.1002/jbm4.10352

Kittaka, M., Yoshimoto, T., Schlosser, C., Rottapel, R., Kajiya, M., Kurihara, H., Reichenberger, E. J., & Ueki, Y. (2019). Alveolar bone protection by targeting the SH3BP2-SYK axis in osteoclasts. *Journal of Bone and Mineral Research*, *35*(2), 382–395. https://doi.org/10.1002/jbmr.3882

Levy, M., Kolodziejczyk, A. A., Thaiss, C. A., & Elinav, E. (2017). Dysbiosis and the immune system. *Nature Reviews Immunology*, *17*(4), 219–232. https://doi.org/10.1038/nri.2017.7

Long, L. L., Svenson, K. L., Mourino, A. J., Michaud, M., Fahey, J. R., Waterman, L., Vandegrift, K. L., & Adams, M. D. (2021). Shared and distinctive features of the gut microbiome of C57BL/6 mice from different vendors and production sites, and in response to a new vivarium. *Lab Animal*, *50*(7), 185–195. https://doi.org/10.1038/s41684-021-00777-0

Papapanou, P. N., Sanz, M., Buduneli, N., Dietrich, T., Feres, M., Fine, D. H., Flemmig, T. F., Garcia, R., Giannobile, W. V., Graziani, F., Greenwell, H., Herrera, D., Kao, R. T., Kebschull, M., Kinane, D. F., Kirkwood, K. L., Kocher, T., Kornman, K. S., Kumar, P. S., … Tonetti, M. S. (2018). Periodontitis: Consensus report of workgroup 2 of the 2017 World Workshop on the Classification of Periodontal and Peri-Implant Diseases and Conditions. *Journal of Clinical Periodontology*, *45*(Suppl 20), S162–S170. https://doi.org/10.1111/jcpe.12946

Payne, M. A., Hashim, A., Alsam, A., Joseph, S., Aduse-Opoku, J., Wade, W. G., & Curtis, M. A. (2019). Horizontal and vertical transfer of oral microbial dysbiosis and periodontal disease. *Journal of Dental Research*, *98*(13), 1503–1510. https://doi.org/10.1177/0022034519877150

Quast, C., Pruesse, E., Yilmaz, P., Gerken, J., Schweer, T., Yarza, P., Peplies, J., & Glockner, F. O. (2013). The SILVA ribosomal RNA gene database project: Improved data processing and web-based tools. *Nucleic Acids Research*, *41*, D590–D596. https://doi.org/10.1093/nar/gks1219

Rausch, P., Basic, M., Batra, A., Bischoff, S. C., Blaut, M., Clavel, T., GlãSner, J., Gopalakrishnan, S., Grassl, G. A., Ganther, C., Haller, D., Hirose, M., Ibrahim, S., Loh, G., Mattner, J., Nagel, S., Pabst, O., Schmidt, F., Siegmund, B., … Baines, J. F. (2016). Analysis of factors contributing to variation in the C57BL/6J fecal microbiota across German animal facilities. *International Journal of Medical Microbiology*, *306*(5), 343–355. https://doi.org/10.1016/j.ijmm.2016.03.004

Rognes, T., Flouri, T., Nichols, B., Quince, C., & Mahe, F. (2016). VSEARCH: A versatile open source tool for metagenomics. *PeerJ*, *4*, e2584. https://doi.org/10.7717/peerj.2584

Schloss, P. D., Westcott, S. L., Ryabin, T., Hall, J. R., Hartmann, M., Hollister, E. B., Lesniewski, R. A., Oakley, B. B., Parks, D. H., Robinson, C. J., Sahl, J. W., Stres, B., Thallinger, G. G., Van Horn, D. J., & Weber, C. F. (2009). Introducing mothur: Open-source, platform-independent, community-supported software for describing and comparing microbial communities. *Applied and Environmental Microbiology*, *75*(23), 7537–7541. https://doi.org/10.1128/AEM.01541-09

Segata, N., Izard, J., Waldron, L., Gevers, D., Miropolsky, L., Garrett, W. S., & Huttenhower, C. (2011). Metagenomic biomarker discovery and explanation. *Genome Biology*, *12*(6), R60. https://doi.org/10.1186/gb-2011-12-6-r60

Tiffany, C. R., & Baumler, A. J. (2019). Dysbiosis: From fiction to function. *American Journal of Physiology Gastrointestinal and Liver Physiology*, *317*(5), G602–G608. https://doi.org/10.1152/ajpgi.00230.2019

Tsukasaki, M., Komatsu, N., Nagashima, K., Nitta, T., Pluemsakunthai, W., Shukunami, C., Iwakura, Y., Nakashima, T., Okamoto, K., & Takayanagi, H. (2018). Host defense against oral microbiota by bone-damaging T cells. *Nature Communication*, *9*(1), 701. https://doi.org/10.1038/s41467-018-03147-6

Wang, Q., Garrity, G. M., Tiedje, J. M., & Cole, J. R. (2007). Naive Bayesian classifier for rapid assignment of rRNA sequences into the new bacterial taxonomy. *Applied and Environmental Microbiology*, *73*(16), 5261–5267. https://doi.org/10.1128/AEM.00062-07

Williams, D. W., Vuong, H. E., Kim, S., Lenon, A., Ho, K., Hsiao, E. Y., Sung, E. C., & Kim, R. H. (2020). Indigenous microbiota protects against inflammation-induced osteonecrosis. *Journal of Dental Research*, *99*(6), 676–684. https://doi.org/10.1177/0022034520908594

You, X., Dadwal, U. C., Lenburg, M. E., Kacena, M. A., & Charles, J. F. (2022). Murine gut microbiome meta-analysis reveals alterations in carbohydrate metabolism in response to aging. *mSystems*, *7*(2), e0124821. https://doi.org/10.1128/msystems.01248-21

Zheng, X., Tizzano, M., Redding, K., He, J., Peng, X., Jiang, P., Xu, X., Zhou, X., & Margolskee, R. F. (2019). Gingival solitary chemosensory cells are immune sentinels for periodontitis. *Nature Communication*, *10*(1), 4496. https://doi.org/10.1038/s41467-019-12505-x

SUPPORTING INFORMATION

Additional supporting information can be found online in the Supporting Information section at the end of this article.

How to cite this article: Arce, M., Endo, N., Dutzan, N., & Abusleme, L. (2022). A reappraisal of microbiome dysbiosis during experimental periodontitis. *Molecular Oral Microbiology*, 1–16. https://doi.org/10.1111/omi.12382